

Cost Modeling for Wastewater Treatment by Using a Packed-bed Electrode Reactor (PBER)

Lizhang Wang^{1,2}, Yan Kong¹, Dongyang Wei³, Ying Kong¹, Peng Li⁴, Xinmei Jiao¹

¹ School of Environment Science and Spatial Informatics, China University of Mining and Technology, Xuzhou City, Jiangsu 221116, PR China;

² NUS Environmental Research Institute, National University of Singapore, 5A Engineering Drive 1, 117411, Singapore;

³ South China Institute of Environmental Sciences, the Ministry of Environmental Protection (MEP) of PR China, Guangzhou City, Guangdong 510655, PR China;

⁴ School of Water Resource & Environmental Engineering, East China Institute of Technology, Nanchang, Jiangxi 330013, PR China

*E-mail: wlzh0731@126.com

Received: 3 May 2017 / Accepted: 1 July 2017 / Published: 13 August 2017

A cost model is presented to predict the power consumption and the demanded electrode area of a packed-bed electrode reactor (PBER) during wastewater treatment. The experimental results from oxidation of organic pollutants in ribonucleic acid (RNA) manufacturing wastewater on an IrO₂-Ta₂O₅/Ti anode show high agreement with model prediction, directly verifying rationality of the proposed model. Hence, the presented kinetics can provide a new approach for accurate estimation of electro-oxidation and a useful tool for cell design during electrochemical wastewater treatment by using the PBER.

Keywords: wastewater treatment; cost modeling; packed-bed electrode reactor (PBER); power consumption; demanded electrode area

1. INTRODUCTION

Recently, electrochemical processes have attracted much attention of researchers in environmental field and have been introduced in treating various industrial wastewaters [1-3]. To increase space-time yield cell configuration with three-dimensional electrode structures e.g. packed-bed electrode reactor (PBER) is developed so as to make reaction take place at low current density and this type framework is being increasingly considered as alternative of achieving required removal of

organic pollutants in wastewaters [4-7]. However, it must be concerned that the overall cost should be well determined in order to evaluate the real feasibility of this technology. It is known that the cost during electrochemical wastewater treatment is composed of power consumption and demanded electrode area associated with running cost and capital investment, respectively at certain chemical oxygen demand (COD) removal efficiency; thus, accurate prediction of the two issues becomes central view of solving this problem. The reported works show that many achievements have been obtained in this area over the past decades, for a merely anodic oxidation, Panizza et. al [8] proposed a model for cost estimation during phenol degradation on boron-doped diamond (BDD) anode, we also has been working towards development of a universal kinetics to predict COD and cost changes over all anode materials [9]. Despite wide use of the PBER in wastewater treatment, few studies on its overall cost are present in the literature. In a previous paper, a mathematical model that can describe COD evolution with reaction time using a PBER equipped with PbO_2/Ti and $\text{IrO}_2\text{-Ta}_2\text{O}_5/\text{Ti}$ anodes has been established and the theoretical results could satisfactorily match the experimental data during phenol elimination and treatment of real industrial wastewaters [10].

With the purpose of helping in overall cost evaluation for electrochemical wastewater treatment, a theoretical model is proposed to use as a design strategy for prediction of the power consumption and demanded electrode area according to the presented COD evolution kinetics. A detail verification of rationality of the model is also provided through ribonucleic acid (RNA) manufacturing wastewater treatment in a PBER at different applied current densities.

2. EXPERIMENTAL SECTION

2.1. Experimental set-up

The process was composed of eight quadrangular reactors constructed by acrylic plexiglass and a D.C. power (model: KZD300/12) having capacity of 0-300 A/0-12 V. Each reactor with 100×50×150 mm dimension was equipped with a pair of $\text{IrO}_2\text{-Ta}_2\text{O}_5/\text{Ti}$ and Ti plates with geometrical area of 0.01 m^2 (100×100 mm) as anode and cathode, respectively and approximately 350 g granular activated carbon (GAC) packed into electrode gap up to a height of about 100 mm. Prior to experiments, GAC with an average particle size of 5.0 mm was washed several times by distilled water to remove fines, oven-dried at 105 °C for 2 days to a constant weight. In addition, a micropore plate installed at bottom of the reactor was employed as a supporter for GAC and electrodes, as well as a solution distributor for even distribution of influent. Peristaltic pumps were used to pump the raw wastewater into each reactor and detail information of the process was shown elsewhere [11].

2.2. Wastewater pre-treatment

Ribonucleic acid (RNA) manufacturing wastewater was used in this study and it was obtained from a sugar factory located in South China. The average COD and pH values are 15000 mg/L and 2.28, and NaCl content is higher than 2.0% (*w/w*). Before electrochemical treatment, the solution pH

was adjusted by sodium hydroxide (NaOH) to neutral state and coagulation by polyaluminium chloride (PAC) with dosage of 3.0 g/L was carried out to eliminate suspended solid (SS) in order to avoid GAC blockage. Then, the solution with average COD value of about 9500 mg/L was treated using the PBER under continuous flow mode at room temperature.

2.3. Analytical methods

All samples were filtered by quartz sand filtration to removal any trace of carbon and then the COD was analyzed by standard method [12]. COD content was used for calculation of experimental current efficiency η and power consumption E_{sp} during wastewater treatment:

$$\eta = \frac{FQ[\text{COD}_0 - \text{COD}(t)]}{8(\gamma + \beta)z_0 \int_0^{y_0} i_M dy} \tag{1}$$

$$E_{sp} = \frac{Uz_0 \int_0^{y_0} i_M dy}{Q[\text{COD}_0 - \text{COD}(t)]} \tag{2}$$

where F is Faraday’s constant; Q the flow rate; COD_0 and $\text{COD}(t)$ the COD values initially and at time t , respectively; γ, β the fractional current utilization ratio of metallic and particulate anode; z_0 and y_0 the electrode width and height; y the flow-by distance of solution at time t ; i_M the current density; U the applied voltage.

The γ, β values could be calculated by the experimental data within a charge transfer control (CTC) regime that meet the relationship of $i_M < 4Fk_m \text{COD}(t)$ (k_m denotes the mass transfer coefficient) by anodic oxidation and treatment in a PBER, as the following forms, respectively

$$\gamma = \frac{FQ[\text{COD}_0 - \text{COD}(t)]}{8z_0 \int_0^{y_0} i_M dy} \tag{3}$$

$$\beta = \frac{FQ[\text{COD}_0 - \text{COD}(t)]}{8z_0 \int_0^{y_0} i_M dy} - \gamma \tag{4}$$

To effectively determine the reaction regimes during RNA manufacturing wastewater treatment, the k_m value was obtained by the following equation [10]:

$$k_m = \sqrt{\frac{i_M Sc^{1/3} D}{nFc_0 \varepsilon d_p (H_R / y_0)^\chi}} (0.765 \text{Re}^{0.18} + 0.345 \text{Re}^{0.614}) \tag{5}$$

where D is the diffusion coefficient, n the electrons transferred in oxidation, c_0 the initial concentration, H_R the cell hydraulic radius, ε the porosity of PBER, d_p the GAC particle diameter; Sc and Re refer to Schmidt and Reynolds numbers, respectively; χ represents the influence factor, which is associated with the cell dimensions and kinds of organic compounds.

Eq. (6) was used to calculate F -test results between experimental data and model simulation.

$$F = \frac{pf_2}{sf_1} \tag{6}$$

where p and s are the regression sum of squares and residual sum of squares, respectively; f_1 the number of independent variable and f_2 the degrees of freedom of parameter s . If the F value is larger than that of $10f_\alpha(f_1, f_2)$ the results are significant at α significance level.

3. MODELING

A mathematical model for prediction of COD evolutions with reaction time during wastewater treatment by a PBER was proposed in a published paper [10]. This kinetics was achieved according to relationship between the limiting current density i_{lim} and the applied one i_{app} that permits to divide the reaction regimes into three stages i.e. CTC, mixed-phase control (MPC) and mass transfer control (MTC) and the model equations under overall conditions are listed in Table 1.

The average current efficiency η is a very important parameter because it determines the theoretical description of the power consumption and demanded electrode area S through the following equations:

$$E_{sp} = \frac{U}{3600} \cdot \frac{nF}{(\gamma + \beta)} \cdot \frac{1}{\eta} \tag{7}$$

$$S = \frac{QX}{(\gamma + \beta)\alpha k_m} \cdot \frac{1}{\eta} \tag{8}$$

Meanwhile, η value can be obtained from the integration of the instantaneous current efficiency (ICE) during electrolysis time (τ) necessary to reach target COD removal efficiency X [8]:

$$\eta = \frac{\int_0^\tau ICE(t)dt}{\tau} \tag{9}$$

At the same time, the equation of ICE with overall conditions is given by

$$\text{for } \gamma \geq \beta/\lambda, \text{ ICE} = \begin{cases} \frac{\alpha\gamma c_0 + \alpha\beta c_0}{(\gamma + \beta)\alpha c_0}, \gamma i_M, i_p < i_{lim} \\ \frac{c(t) + \alpha\beta c_0}{(\gamma + \beta)\alpha c_0}, \gamma i_M \geq i_{lim} > i_p \\ \frac{(1 + \lambda)c(t)}{(\gamma + \beta)\alpha c_0}, \gamma i_M, i_p \geq i_{lim} \end{cases} \text{ or for } \gamma < \beta/\lambda, \text{ ICE} = \begin{cases} \frac{\alpha\gamma c_0 + \alpha\beta c_0}{(\gamma + \beta)\alpha c_0}, \gamma i_M, i_p < i_{lim} \\ \frac{\alpha\gamma c_0 + \lambda c(t)}{(\gamma + \beta)\alpha c_0}, i_p \geq i_{lim} > \gamma i_M \\ \frac{(1 + \lambda)c(t)}{(\gamma + \beta)\alpha c_0}, \gamma i_M, i_p \geq i_{lim} \end{cases} \tag{10}$$

Table 1. The proposed ³SRT model under different applied current density in case of $\gamma \geq \beta/\lambda$ and $\gamma < \beta/\lambda$.

Condition	α ranges	CTC	MPC	MTC
$\gamma \geq \beta/\lambda$	(0, 1/ γ)	$c(t) = c_0[1 - (\gamma + \beta) \frac{\alpha k_m t}{\epsilon x_0}]$	$c(t) = \alpha c_0 \left\{ (\gamma + \beta) \exp\left[-\frac{k_m t}{\epsilon x_0} + \frac{(1 - \gamma\alpha)}{\alpha(\gamma + \beta)}\right] - \beta \right\}$	$c(t) = \left[\frac{\lambda(\gamma + \beta)}{\beta(1 + \lambda)}\right]^{(1+\lambda)} \frac{\alpha\beta c_0}{\lambda} \exp\left[-(1 + \lambda) \frac{k_m t}{\epsilon x_0} + \frac{(1 - \gamma\alpha)(1 + \lambda)}{\alpha(\gamma + \beta)}\right]$
	[1/ γ , λ/β)		$c(t) = \alpha c_0 \left[\left(\frac{1}{\alpha} + \beta\right) \exp\left(-\frac{k_m t}{\epsilon x_0}\right) - \beta\right]$	$c(t) = \left[\frac{\lambda(1 + \alpha\beta)}{\alpha\beta(1 + \lambda)}\right]^{(1+\lambda)} \frac{\alpha\beta c_0}{\lambda} \exp\left[-(1 + \lambda) \frac{k_m t}{\epsilon x_0}\right]$
	[λ/β , + ∞)			$c(t) = c_0 \exp\left[-(1 + \lambda) \frac{k_m t}{\epsilon x_0}\right]$
$\gamma < \beta/\lambda$	(0, λ/β)	$c(t) = c_0[1 - (\gamma + \beta) \frac{\alpha k_m t}{\epsilon x_0}]$	$c(t) = \frac{\alpha c_0}{\lambda} \left\{ (\gamma + \beta) \exp\left[-\frac{\lambda k_m t}{\epsilon x_0} + \frac{(\lambda - \alpha\beta)}{\alpha(\gamma + \beta)}\right] - \gamma \right\}$	$c(t) = \alpha\gamma c_0 \left[\frac{(\gamma + \beta)}{\gamma(1 + \lambda)}\right]^{(1+1/\lambda)} \exp\left[-(1 + \lambda) \frac{k_m t}{\epsilon x_0} + \frac{(\lambda - \alpha\beta)(1 + \lambda)}{\alpha\lambda(\gamma + \beta)}\right]$
	[λ/β , 1/ γ)		$c(t) = \frac{\alpha c_0}{\lambda} \left[\left(\gamma + \frac{\lambda}{\alpha}\right) \exp\left(-\frac{\lambda k_m t}{\epsilon x_0}\right) - \gamma\right]$	$c(t) = \alpha\gamma c_0 \left[\frac{(\alpha\gamma + \lambda)}{\alpha\gamma(1 + \lambda)}\right]^{(1+1/\lambda)} \exp\left[-(1 + \lambda) \frac{k_m t}{\epsilon x_0}\right]$
	[1/ γ , + ∞)			$c(t) = c_0 \exp\left[-(1 + \lambda) \frac{k_m t}{\epsilon x_0}\right]$

Note: $\alpha = i_M/nFk_m c_0$, where k_m is the mass transfer coefficient, c_0 the initial concentration; λ denotes the expansion factor of the bed electrode, $\lambda = A_p/A_M$, where A_p, A_M are area of the particulate and metallic electrodes, respectively.

Accordingly, Eqs. (7)–(10) and the equations in Table 1 result into achievements of theoretical description of the cost model for electrochemical treatment of organic pollutants.

Case I: Three stages ($\alpha \in (0, 1/\gamma)$ or $(0, \lambda/\beta)$)

(i) One regime: $\gamma i_M, i_P < i_{lim}$.

There is only CTC regime across the whole bed electrode. The η and ICE are in the same value of 1.0, i.e.

$$\eta = \text{ICE} = 1.0 \tag{11}$$

Therefore, substituting Eq. (11) into Eqs. (7) and (8), respectively, we can obtain

$$E_{sp} = \frac{U}{3600} \cdot \frac{nF}{(\gamma + \beta)} \tag{12}$$

$$S = \frac{QX}{(\gamma + \beta)\alpha k_m} \tag{13}$$

(ii) Two regimes: $\gamma i_M \geq i_{lim} > i_P$ or $i_P \geq i_{lim} > \gamma i_M$.

The oxidation is in CTC initially and MPC subsequently, and the description of η follows:

$$\eta = \frac{X}{1 - \gamma\alpha [1 + (1 + \beta/\gamma) \ln \frac{1 - X + \alpha\beta}{(\gamma + \beta)\alpha}]} \tag{14}$$

Simple rearrangement of Eqs.(14), (7) and (8) provides

$$E_{sp} = \frac{U}{3600} \cdot \frac{nF}{(\gamma + \beta)X} \cdot \left\{ 1 - \gamma\alpha [1 + (1 + \beta/\gamma) \ln \frac{1 - X + \alpha\beta}{(\gamma + \beta)\alpha}] \right\} \tag{15}$$

$$S = \frac{Q}{(\gamma + \beta)\alpha k_m} \cdot \left\{ 1 - \gamma\alpha [1 + (1 + \beta/\gamma) \ln \frac{1 - X + \alpha\beta}{(\gamma + \beta)\alpha}] \right\} \tag{16}$$

As for $\gamma < \beta/\lambda$, the η is shown as

$$\eta = \frac{X}{1 - \frac{\alpha\beta}{\lambda} [1 + (1 + \gamma/\beta) \ln \frac{\lambda - \lambda X + \alpha\gamma}{(\gamma + \beta)\alpha}]} \tag{17}$$

Then, Eqs (18) and (19) could be employed to calculate the E_{sp} and S for this condition.

$$E_{sp} = \frac{U}{3600} \cdot \frac{nF}{(\gamma + \beta)X} \cdot \left\{ 1 - \frac{\alpha\beta}{\lambda} [1 + (1 + \gamma/\beta) \ln \frac{\lambda - \lambda X + \alpha\gamma}{(\gamma + \beta)\alpha}] \right\} \tag{18}$$

$$S = \frac{Q}{(\gamma + \beta)\alpha k_m} \cdot \left\{ 1 - \frac{\alpha\beta}{\lambda} [1 + (1 + \gamma/\beta) \ln \frac{\lambda - \lambda X + \alpha\gamma}{(\gamma + \beta)\alpha}] \right\} \tag{19}$$

(iii) Three regimes: $\gamma i_M, i_P \geq i_{lim}$.

The three different regimes appear with the regular order of CTC, MPC and MTC during oxidation of the organic compounds. In case of $\gamma \geq \beta/\lambda$, taking into account the above equations, it can be easily shown that

$$\eta = \frac{X}{1 - \gamma\alpha \left\{ 1 + \frac{(\gamma + \beta)}{\gamma(1 + \lambda)} \ln \left[\left(\frac{\beta}{\lambda} \right)^\lambda \left(\frac{1 + \lambda}{\gamma + \beta} \right)^{(1 + \lambda)} \frac{1 - X}{\alpha} \right] \right\}} \tag{20}$$

The E_{sp} and S can be obtained by combination of Eqs. (20), (7) and (8), i.e.

$$E_{sp} = \frac{U}{3600} \cdot \frac{nF}{(\gamma + \beta)X} \cdot \left(1 - \gamma\alpha \left\{ 1 + \frac{(\gamma + \beta)}{\gamma(1 + \lambda)} \ln \left[\left(\frac{\beta}{\lambda} \right)^\lambda \left(\frac{1 + \lambda}{\gamma + \beta} \right)^{(1 + \lambda)} \frac{1 - X}{\alpha} \right] \right\} \right) \tag{21}$$

$$S = \frac{Q}{(\gamma + \beta)\alpha k_m} \cdot \left(1 - \gamma\alpha \left\{ 1 + \frac{(\gamma + \beta)}{\gamma(1 + \lambda)} \ln \left[\left(\frac{\beta}{\lambda} \right)^\lambda \left(\frac{1 + \lambda}{\gamma + \beta} \right)^{(1 + \lambda)} \frac{1 - X}{\alpha} \right] \right\} \right) \tag{22}$$

When $\gamma < \beta/\lambda$, the equations for calculation of η , E_{sp} and S are as following

$$\eta = \frac{X}{1 - \alpha \left\{ \frac{\beta}{\lambda} + \frac{(\gamma + \beta)}{(1 + \lambda)} \ln \left[(\gamma)^{1/\lambda} \left(\frac{1 + \lambda}{\gamma + \beta} \right)^{(1+1/\lambda)} \frac{1 - X}{\alpha} \right] \right\}} \quad (23)$$

$$E_{sp} = \frac{U}{3600} \cdot \frac{nF}{(\gamma + \beta)X} \cdot \left(1 - \alpha \left\{ \frac{\beta}{\lambda} + \frac{(\gamma + \beta)}{(1 + \lambda)} \ln \left[(\gamma)^{1/\lambda} \left(\frac{1 + \lambda}{\gamma + \beta} \right)^{(1+1/\lambda)} \frac{1 - X}{\alpha} \right] \right\} \right) \quad (24)$$

$$S = \frac{Q}{(\gamma + \beta)\alpha k_m} \cdot \left(1 - \alpha \left\{ \frac{\beta}{\lambda} + \frac{(\gamma + \beta)}{(1 + \lambda)} \ln \left[(\gamma)^{1/\lambda} \left(\frac{1 + \lambda}{\gamma + \beta} \right)^{(1+1/\lambda)} \frac{1 - X}{\alpha} \right] \right\} \right) \quad (25)$$

Case II: Two stages ($\alpha \in [1/\gamma, \lambda/\beta]$ or $[\lambda/\beta, 1/\gamma]$)

(i) One regime: $\gamma i_M \geq i_{lim} > i_P$ or $i_P \geq i_{lim} > \gamma i_M$.

The whole system is in MPC and the same method allows one to obtain

$$\eta = \frac{X}{\alpha(\gamma + \beta) \ln \frac{(1 + \alpha\beta)}{(1 + \alpha\beta - X)}}, \text{ for } \gamma \geq \beta/\lambda \quad (26)$$

and

$$\eta = \frac{\lambda X}{\alpha(\gamma + \beta) \ln \frac{(\lambda + \alpha\gamma)}{(\lambda + \alpha\gamma - \lambda X)}}, \text{ for } \gamma < \beta/\lambda \quad (27)$$

Similarly, we can get

$$E_{sp} = \frac{\alpha nFU}{3600X} \cdot \ln \frac{(1 + \alpha\beta)}{(1 + \alpha\beta - X)} \quad (28)$$

$$S = \frac{Q}{k_m} \cdot \ln \frac{(1 + \alpha\beta)}{(1 + \alpha\beta - X)} \quad (29)$$

$$E_{sp} = \frac{\alpha nFU}{3600\lambda X} \cdot \ln \frac{(\lambda + \alpha\gamma)}{(\lambda + \alpha\gamma - \lambda X)} \quad (30)$$

$$S = \frac{Q}{k_m \lambda} \cdot \ln \frac{(\lambda + \alpha\gamma)}{(\lambda + \alpha\gamma - \lambda X)} \quad (31)$$

Eqs. (28), (29) and (30), (31) are suitable for the condition of $\gamma \geq \beta/\lambda$ and $\gamma < \beta/\lambda$, respectively.

(ii) Two regimes: $\gamma i_M, i_P \geq i_{lim}$.

The bed electrode is determined by MPC and MTC regimes. In case of $\gamma \geq \beta/\lambda$, it is clear that

$$\eta = \frac{X}{\frac{\alpha(\gamma + \beta)}{(1 + \lambda)} \ln \left(\left[\frac{\lambda(1 + \alpha\beta)}{\alpha\beta(1 + \lambda)} \right]^{(1+\lambda)} \frac{\alpha\beta}{\lambda(1 - X)} \right)} \quad (32)$$

The E_{sp} and S can be calculated by

$$E_{sp} = \frac{\alpha nFU}{3600(1 + \lambda)X} \cdot \ln \left(\left[\frac{\lambda(1 + \alpha\beta)}{\alpha\beta(1 + \lambda)} \right]^{(1+\lambda)} \frac{\alpha\beta}{\lambda(1 - X)} \right) \quad (33)$$

$$S = \frac{Q}{(1 + \lambda)k_m} \cdot \ln \left(\left[\frac{\lambda(1 + \alpha\beta)}{\alpha\beta(1 + \lambda)} \right]^{(1+\lambda)} \frac{\alpha\beta}{\lambda(1 - X)} \right) \quad (34)$$

While when $\gamma < \beta/\lambda$, combination of the corresponding equations will yield

$$\eta = \frac{X}{\frac{\alpha(\gamma + \beta)}{(1 + \lambda)} \ln \left(\left[\frac{(\alpha\gamma + \lambda)}{\alpha\gamma(1 + \lambda)} \right]^{(1+1/\lambda)} \frac{\alpha\gamma}{1 - X} \right)} \quad (35)$$

$$E_{sp} = \frac{\alpha nFU}{3600(1 + \lambda)X} \cdot \ln \left(\left[\frac{(\alpha\gamma + \lambda)}{\alpha\gamma(1 + \lambda)} \right]^{(1+1/\lambda)} \frac{\alpha\gamma}{1 - X} \right) \quad (36)$$

$$S = \frac{Q}{(1 + \lambda)k_m} \cdot \ln \left(\left[\frac{(\alpha\gamma + \lambda)}{\alpha\gamma(1 + \lambda)} \right]^{(1+1/\lambda)} \frac{\alpha\gamma}{1 - X} \right) \quad (37)$$

Case III: One stages ($\alpha \in [\lambda/\beta, +\infty)$ or $[1/\gamma, +\infty)$)

During this process, only MTC regime is considered, thus

$$\eta = -\frac{(1 + \lambda)X}{\alpha(\gamma + \beta)\ln(1 - X)} \tag{38}$$

The E_{sp} and S act as

$$E_{sp} = -\frac{\alpha n F U \ln(1 - X)}{3600(1 + \lambda)X} \tag{39}$$

$$S = -\frac{Q \ln(1 - X)}{(1 + \lambda)k_m} \tag{40}$$

4. RESULTS AND DISCUSSION

According to the equations in Table 1 and reported kinetics for anodic oxidation [13, 14], the COD variations are independent of reaction time in the CTC regime, i.e. the space-time yield should be parallel to time axis. Further based on Eq. (1), we could infer that the intervals on y-axis equate to values of γ and $(\gamma + \beta)$ for anodic oxidation and PBER, respectively. At the same time, if oxidation is in MTC regime, an exponential decrease of COD is found thus effectively assigning value of parameter λ . Fig. 1 shows the results calculated by Eq. (1) and COD variation with time during RNA manufacturing wastewater treatment. From this figure, we can observe that trend lines of the experimental data are parallel to the abscissa axis and they are with average values of 0.39 and 1.00 for anodic oxidation and PBER when the reaction time is less than about 2.0 h, respectively (Fig. 1a). The duration of CTC regimes calculated using theoretical equations are 14.47 h and 2.48 h, permitting to obtain the parameters γ and β with values of 0.39 and 0.61, respectively. Similarly, first-order kinetics can provide a satisfactory regression of experimental data obtained at i_M of 200 A/m² and Q of 0.2 L/h, which gives λ with value of 1.11 (Fig. 1b). The same phenomenon were widely illustrated in treatment of landfill leachate [15], phenol [16] and 4,4'-diaminostilbene-2,2'-disulfonic (DSD) acid manufacturing wastewater [17].

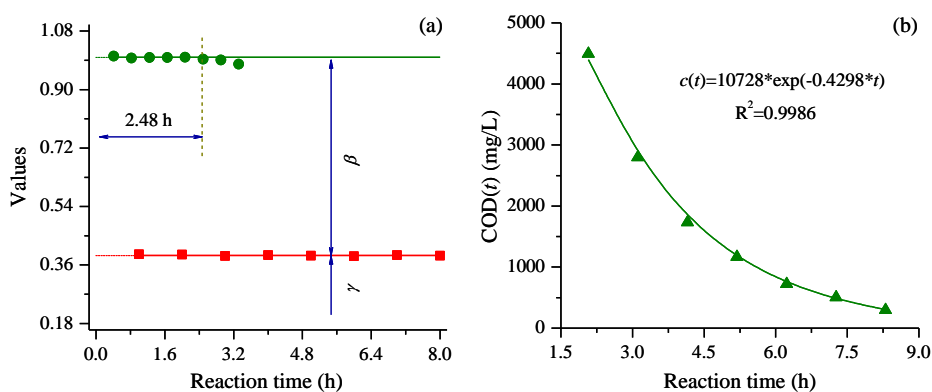
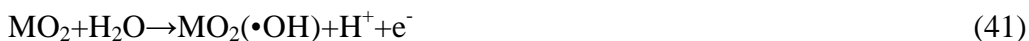


Figure 1. The achievement of γ , β and λ values during RNA manufacturing wastewater treatment at $i_M=120$ A/m², $Q=0.6$ L/h and $[COD]_0=9640$ mg/L (a) and $i_M=200$ A/m², $Q=0.2$ L/h and $[COD]_0=9536$ mg/L in the PBER (b). The symbols \bullet and \blacksquare depict the anodic oxidation and the reaction in the PBER, respectively.

Fig. 2 describes dependence of the COD on reaction time at current densities of 50, 150 and 250 A/m², and flow rate of 0.3 L/h. In a PBER equipped with an IrO₂-Ta₂O₅/Ti anode having lower oxygen evolution potential, absorbed hydroxyl radicals (•OH) and active chlorine could be electrochemically generated, which are responsible for organics degradation [18-20].



Meanwhile, higher current density (voltage) leads to a larger production of these oxidants due to increase of the electric field intensity, thus enhancing COD decay (Fig. 2). And it is worth noting that the effluent COD is only 580 mg/L at reaction time of 5.54 h and i_M of 250 A/m², demonstrating the PBER possesses considerable superiorities such as higher space-time yield, lower reagent cost and less sludge production compared with the membrane bioreactor (MBR) [21], photo-Fenton oxidation [22] and electrocoagulation [23] in treating such kind wastewater. In addition, we observe the model simulation matches the experimental data with higher agreement ($R^2=0.9999, 0.9997$ and 0.9997 at 50, 150 and 250 A/m², respectively), which validates the proposed ³SRT (Table 1) is also suitable for prediction of RNA manufacturing wastewater treatment.

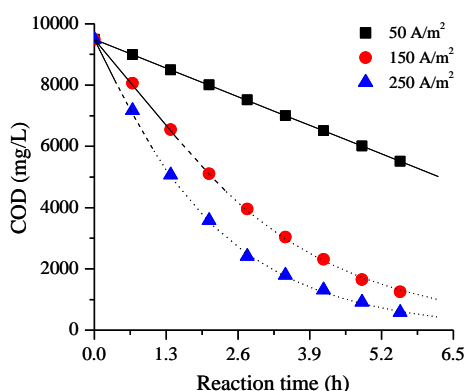


Figure 2. Effect of applied current density on COD changes during RNA manufacturing wastewater treatment in the PBER at $Q=0.3$ L/h and $[\text{COD}]_0=9490$ mg/L. The solid, dashed and dotted lines depict the CTC, MPC and MTC regimes and $\gamma=0.39, \beta=0.61$ and $\lambda=1.11$ are used for model simulation.

The power consumption is directly determined by applied voltage and its minimum theoretical value could be obtained with $\eta=1.0$ and a necessary voltage (U_d) corresponds to generate a net faradic current that approximates to zero [8]. The current and voltage obeys the following relation:

$$U = U_d + I_s R_s \quad (43)$$

where I_s and R_s represent the current and resistance of a single PBER, respectively. Fig. 3 shows the current variation with that of voltage and as can be seen there is a perfect linear relationship of the two parameters with description of $y=3.771 \times x + 2.8989$ ($R^2=0.9999$). Hence, this results in achievement of the minimum E_{sp} (9.71 kWh/kg COD, $U_d=2.8989$) and calculation of voltages at different currents for prediction of power consumption as well.

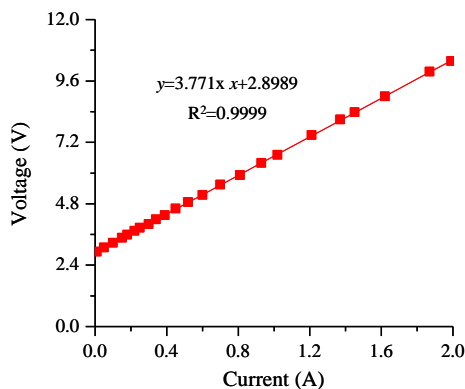


Figure 3. The relationship between applied voltage and current of a single PBER filled with fresh RNA manufacturing wastewater under a steady state.

The dependence of the E_{sp} at current densities of 50, 150 and 250 A/m² on the reaction time is depicted in Fig. 4. The results in Fig. 4a obviously show the experimental E_{sp} under these condition are all higher than the minimum one and less current density leads to lower power consumption closed to the theoretical value (e.g. 16.05 kWh/kg COD at 50 A/m²), illustrating oxidation with very small current would be a feasible strategy for saving power [24]. Furthermore, we can observe the theoretical E_{sp} could satisfactorily match the experimental ones, and the trends of E_{sp} remain a linear relation with time initially, then a slow increase subsequently and an abrupt rise finally, which is for successive appearance of the CTC, MPC and MTC regimes under galvanostatic condition.

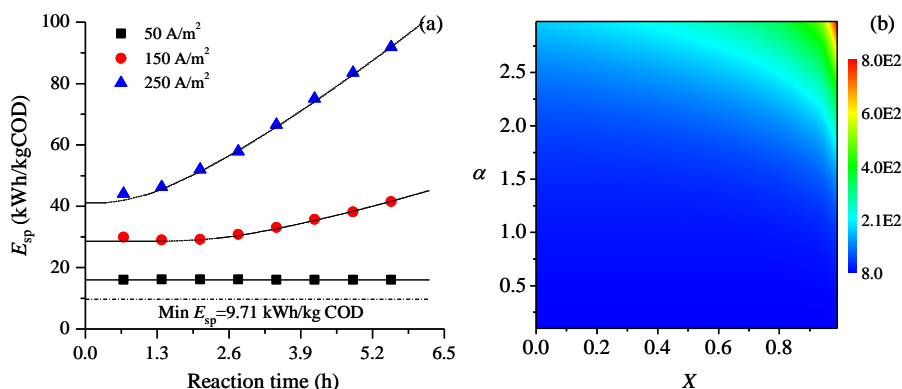


Figure 4. Comparison of experimental results and model prediction on power consumption with reaction time (a) and the E_{sp} simulation against X (b) for different α values (applied current density) during RNA manufacturing wastewater treatment using the PBER. The notation and experimental conditions are the same to those of Fig. 2.

The same phenomenon was also observed in *p*-nitrophenol oxidation on RuO₂/Ti anode and landfill leachate treatment on boron-doped diamond electrode [25, 26]. Moreover, the rationality of the proposed equations for power consumption estimation is completely confirmed by higher regression coefficients ($R^2=0.9941$ and 0.9986) and considerable *F*-test results at a significance level of 99%

($F=439.9$ and 2040) between the experimental data and model calculation at these applied current densities except 50 A/m^2 .

Taking into account the above analysis, the presented equations could naturally provide prediction of E_{sp} under different current density and COD removal efficiency and the simulated results are described by Fig. 4b. Lower α and X values bring about less power consumption, and vice versa, interpreting the technique is extremely suitable for pre-treatment of concentrated wastewaters or advanced treatment of solutions with low COD values. Nevertheless, the E_{sp} value is still could be acceptable even if the COD removal efficiency is relatively higher; taken X of 0.95 for an example, E_{sp} with values of 9.84 and 151 kWh/kg COD are obtained at α of 0.1 (1 A/m^2) and 1.87 (350 A/m^2), respectively and the latter is 15.3 times of the former, which strongly validates the superiority of less α value in power reduction.

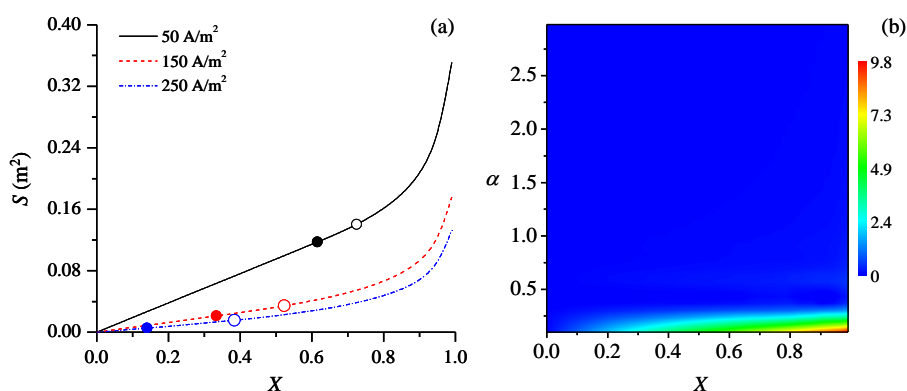


Figure 5. Theoretical trends of demanded electrode area at the given three current densities (b) and the S simulation against X for different α values (b). The values of X_{CrP} and X_{CrM} are calculated by equations of $(1-\beta\alpha/\lambda)$ and $(1-\gamma\alpha)$ and they are described by full and open circles in Fig. 5a. The experimental conditions are the same to those of Fig. 4.

Fig. 5 illustrates the theoretical trends of the demanded electrode area as a function of COD removal efficiency at different α values. A linear increase of S with X is initially achieved until the critical COD removal on particulate electrode (X_{CrP}) and afterwards they follow a significant non-linear increase (Fig. 5a). Contrary to the power consumption, increase of α value (i.e. raising applied current density) could effectively reduce the demanded electrode area; still taking X of 0.95 for an example, we can obtain the S values of 9.06 and 0.07 m^2 at α of 0.1 and 1.87 , respectively, and the results indicate higher α (larger applied current density) is beneficial to decrease investment cost of electrodes. The simulation in Fig. 5b directly provides proof for such a conclusion. Thus, we can acquire that the applied current density plays contradictory roles in power consumption and demanded electrode area and hence to increase or decrease α probably leads to a reduction of either of them but does not mean minimization of the overall cost. For this reason, further research on optimization of the oxidation by using the PBER still should be required by taking into account power cost and capital investment.

5. CONCLUSION

In this work, we propose a theoretical model to estimate operating cost including power consumption (E_{sp}) and demanded electrode area (S) during electro-oxidation of organic compound and the theory has been verified by RNA manufacturing wastewater treatment in a PBER with IrO₂-Ta₂O₅/Ti anode. The experimental results indicate lower applied current density leads to less power consumption, and vice versa. At the same time, the regress analysis and F -test results show very high agreement between model and experimental E_{sp} at all applied current densities. The theoretical simulation illustrates both higher E_{sp} and larger S are required under higher COD removal efficiency; however, an increase of α causes an contradictory issue i.e. increase of power consumption but decrease of demanded electrode area, which is worthy of further studying in optimization of overall cost of wastewater treatment using a PBER.

ACKNOWLEDGEMENTS

The authors wish to acknowledge the financial support by the Fundamental Research Funds for the Central Universities of China (2015XKZD10).

References

1. R.M. Farinos, L.A.M. Ruotolo, *Electrochim. Acta* 224 (2017) 32.
2. S. Youa, B. Liu, Y. Gao, Y. Wang, C.Y. Tang, Y. Huang, N. Ren, *Electrochim. Acta* 214 (2016) 326.
3. B. Wang, Y. Wu, B. Jiang, H. Song, W. Li, Y. Jiang, C. Wang, L. Sun, Q. Li, A. Li, *Electrochim. Acta* 219 (2016) 509.
4. M. Xiao, Y. Zhang, *Chemosphere* 152 (2016) 17.
5. M. Li, F. Zhao, M. Sillanpää, Y. Meng, D. Yin, *Sep. Purif. Technol.* 156 (2015) 588.
6. N. Gedam, N.R. Neti, *J. Environ. Chem. Eng.* 2 (2014) 1527.
7. Z. Wang, J. Qi, Y. Feng, K. Li, X. Li, *J. Ind. Eng. Chem.* 20 (2014) 3672.
8. M. Panizza, P.A. Michaud, G. Cerisola, Ch. Comninellis, *Electrochem. Commun.* 3 (2001) 336.
9. L. Wang, S. Yang, P. Li, Z. Li, Y. Zhao, *Electrochim. Acta* 206 (2016) 270.
10. L. Wang, B. Wu, P. Li, B. Zhang, N. Balasubramanian, Y. Zhao, *Chem. Eng. J.* 284 (2016) 240.
11. L. Wang, Y. Hu, Y. Zhang, P. Li, Y. Zhao, *Sep. Purif. Technol.* 109 (2013) 18.
12. APHA. *Standard methods for examination of water and wastewater*, 20th ed. Washington DC: APHA; 1998.
13. M. Panizza, A. Kapalka, Ch. Comninellis, *Electrochim. Acta* 53 (2008) 2289.
14. A. Kapalka, G. Fóti, Ch. Comninellis, *J. Appl. Electrochem.* 38 (2008) 7.
15. N. N. Rao, M. Rohit, G. Nitin, P.N. Parameswaran, J.K. Astik, *Chemosphere* 76 (2009) 1206.
16. Ch. Comninellis, C. Pulgarin, *J. Appl. Electrochem.* 21 (1991) 703.
17. L. Wang, S. Yang, B. Wu, Z. Li, P. Li, Y. Zhao, *Int. J. Electrochem. Sci.* 11 (2016) 2284.
18. C. Ahmed Basha, R. Saravanathamizhan, V. Nandakumar, K. Chitra, C.W. Lee, *Chem. Eng. Res. Des.* 91 (2013) 552.
19. P. Cañizares, F. Larrondo, J. Lobato, M.-A. Rodrigo, C. Sáez, *J. Electrochem. Soc.* 152 (2005) D191.
20. K.B. Lee, M.B. Gu, S.H. Moon, *Water Res.* 37 (2003) 983.
21. M.J. Nosratpour, M. Sadeghi, K. Karimi, S. Ghesmati, *Adv. Environ. Technol.* 3 (2015) 105.
22. C. Wei, Y. Zhang, C. Wu, C. Hu, *J. Cent. South Univ. Technol.* 13 (2006) 481.

23. M. Kobya, S. Delipinar, *J. Hazard. Mater.* 154 (2008) 1133.
24. P. Piya-areetham, K. Shenchunthichai, M. Hunsom, *Water Res.* 40 (2006) 2857.
25. S. Kumar, S. Singh, V.C. Srivastava, *Chem. Eng. J.* 263 (2015) 135.
26. M. Zolfaghari , K. Jardak , P. Drogui, S.K. Brar, G. Buelna, R. Dubé, *J. Environ. Manage.* 184 (2016) 318.

© 2017 The Authors. Published by ESG (www.electrochemsci.org). This article is an open access article distributed under the terms and conditions of the Creative Commons Attribution license (<http://creativecommons.org/licenses/by/4.0/>).